EPJ Web of Conferences **271**, 07003 (2022) https://doi.org/10.1051/epjconf/202227107003
HYP2022

On K^--nuclear interaction, K^--nuclear quasibound states and K^- atoms

Jaroslava Óbertová[1,*], *Eliahu* Friedman[2], *Jiří* Mareš[3], and *Àngels* Ramos[4]

[1]Faculty of Nuclear Sciences and Physical Engineering, Czech Technical University in Prague, Břehová 7, 11519 Prague, Czech Republic
[2]Racah Institute of Physics, The Hebrew University, 91904 Jerusalem, Israel
[3]Nuclear Physics Institute of the Czech Academy of Sciences, 25068 Řež, Czech Republic
[4]Departament de Física Quàntica i Astrofísica and Institut de Ciències del Cosmos, Universitat de Barcelona, Barcelona, Spain

Abstract. The K^-N potentials derived from SU(3) chiral coupled-channel meson-baryon interaction models fail to describe kaonic atom data. It was shown that K^- single-nucleon potentials have to be supplemented by a phenomenological K^- multi-nucleon optical potential in order to achieve good description of the data. Moreover, only the Prague, Kyoto-Munich and Barcelona models are able to account for the experimental data on K^- atoms and K^- single-nucleon absorption ratios from bubble chamber experiments. A considerable imaginary part coming from the multi-nucleon absorption ruled out existence of narrow K^--nuclear quasibound states in nuclei with $A \geq 6$.
We have developed a microscopic model for the K^-NN absorption in nuclear matter. The absorption was described as a meson-exchange process and the primary K^-N interaction strength was derived from the state-of-the-art chiral models. The medium modifications of the K^-N scattering amplitudes due to the Pauli exclusion principle were taken into account. The model was applied in calculations of kaonic atoms for the first time. The description of the data improved significantly when the two nucleon absorption was considered.

1 K^-N interaction models

The description of low-energy meson-baryon interactions is currently provided by SU(3) chiral coupled-channel meson-baryon interaction models which represent a synergy between the chiral perturbation theory and the coupled channel T-matrix resummation techniques. The chiral models were successfully applied to the description of the K^-N interaction near threshold. The parameters of the models are fitted to K^-p scattering data [1–3], threshold branching ratios [4, 5] and strong-interaction energy shifts and widths in kaonic hydrogen [6]. In Figure 1, there is a comparison of real and imaginary parts of the s-wave free-space K^-p (top panel) and K^-n (bottom panel) scattering amplitudes in the state-of-the-art chiral models. There is a good agreement of the Prague (P) [7], Kyoto-Munich (KM) [8], Murcia (M1 and M2) [9], and Barcelona (BCN) [11] models on the K^-p amplitude at and above threshold since their parameters are fitted to the experimental data in this region. The Bonn

*e-mail: jaroslava.obertova@fjfi.cvut.cz

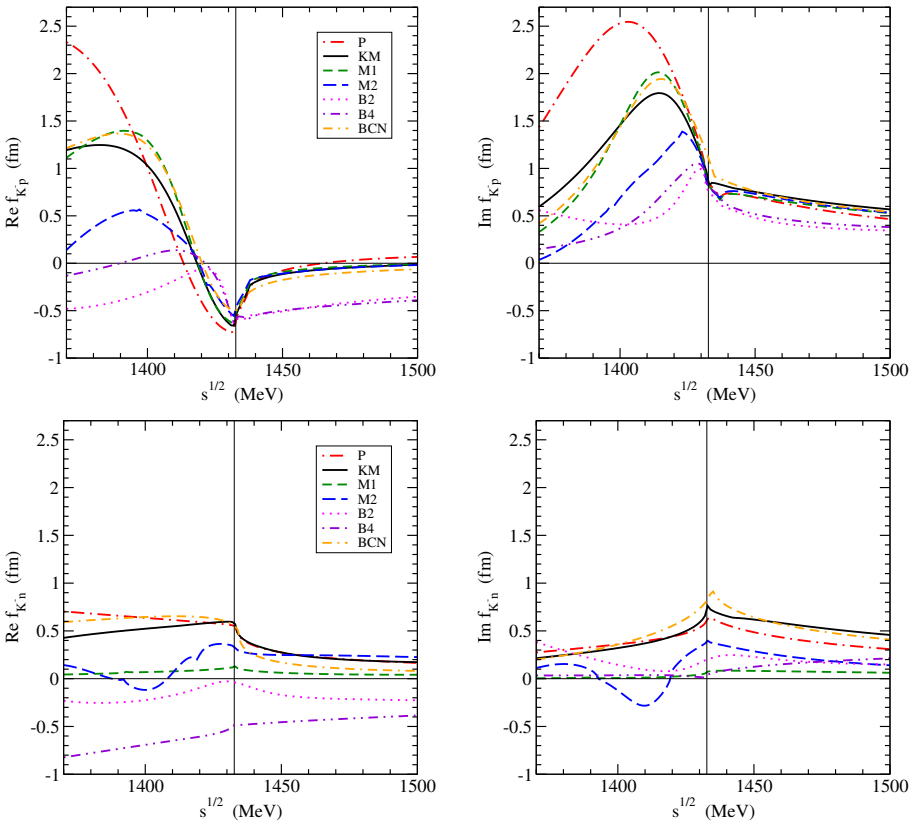

Figure 1. Real (left) and imaginary (right) parts of the s-wave free-space K^-p (top panel) and K^-n (bottom panel) amplitude in the state-of-the-art chiral models.

models (B2 and B4) [10] do not agree with the rest of the models above threshold since higher partial waves were included in the fit. Below threshold the models differ significantly from each other. In the case of the K^-n amplitude, the models do not match each other even at and above threshold due to the lack of sufficiently accurate data. As a consequence, various chiral models yield considerably different K^- optical potentials below threshold.

2 Kaonic atoms and multi-nucleon absorption

A valuable source of information about the K^--nuclear interaction below threshold are kaonic atoms. Their study gives us unique information about the K^--nuclear potential. A sensitive test of any K^-N interaction model is its ability to fit the kaonic atoms data. In Table 1, there are values of $\chi^2(65)$ stemming from the comparison of the results for K^- potentials with the data for all considered chiral models [12]. The values of $\chi^2(65)$ are exceedingly large, implying that K^- optical potentials based on K^- single-nucleon chiral amplitudes are generally unable to fit the kaonic atoms data. The reason for this discrepancy lies in the fact that the considered chiral models do not address the K^- interactions with two and more nucleons. The K^- multi-nucleon absorption represents about 20% of all K^- absorptions in the surface region of atomic nuclei and its role increases with density; its consideration is thus crucial for

Table 1. Values of $\chi^2(65)$ resulting from confrontation of selected chiral K^- optical potentials with kaonic atoms data.

model	B2	B4	M1	M2	P	KM
$\chi^2(65)$	1174	2358	2544	3548	2300	1806

a realistic description of the K^--nucleus interaction. Friedman and Gal [12] supplemented the optical potential constructed from chiral K^-N amplitudes by a phenomenological potential describing the K^- multi-nucleon processes:

$$2\mu_{K^-} V^{\rm phen}_{K^-{\rm multiN}} = -4\pi B(\frac{\rho}{\rho_0})^\alpha \rho \,, \tag{1}$$

where μ_{K^-} is the K^--nucleus reduced mass, ρ is the nuclear density distribution, ρ_0 is the saturation density, and complex amplitude B together with parameter α are fitted to the data. The K^- single-nucleon potentials supplemented by a phenomenological density dependent multi-nucleon term provided considerably better description of kaonic atoms. Equally good fits were achieved for all considered chiral models, with values of $\chi^2(65)$ for all models in the range from 105 to 125 [12].

The analysis of Ref. [12] revealed in addition that only three models supplemented by the phenomenological K^- multi-nucleon potential were able to reproduce simultaneously kaonic atoms data and K^- single-nucleon absorption fraction from old bubble chamber experiments, $\mathrm{BR}_{K^-N} = 0.75 \pm 0.05$ [13–15]. Figure 2 shows the calculated values of K^- single-nucleon absorption fraction for lower (solid lines) and upper (dashed lines) atomic states as a function of the proton number Z for considered chiral models. The gray band denotes the experimental value including the error bar. Only the P, KM, and BCN models are compatible with the data. The compatibility of the three models with the data was confirmed later by the measurement of the $K^-n \to \pi\Lambda$ amplitude by the AMADEUS collaboration [16].

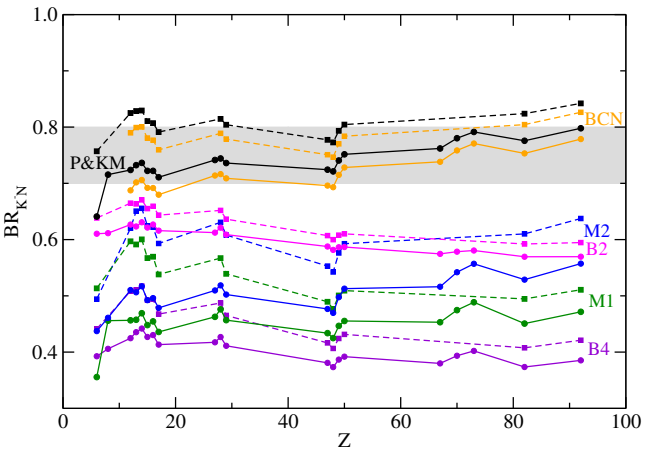

Figure 2. K^- single-nucleon absorption fraction, BR_{K^-N}, calculated for lower (solid lines) and upper (dashed lines) atomic levels using the state-of-the-art chiral models as a function of the proton number Z. The gray band denotes the experimental value including the error bar deduced from bubble chamber experiments [13–15].

3 K^- quasibound states in many-body systems

The attractive nature of K^-N interaction led to conjectures about the existence of K^- bound states in atomic nuclei (see, e.g., [17]). We explored nuclear K^- quasibound states in many-body systems and calculated their binding energies and widths employing the chiral K^- single-nucleon + phen. multi-nucleon optical potential [18, 19]. The K^- single-nucleon potential was derived from the P and KM model amplitudes. In-medium modifications of the amplitudes due to the Pauli correlations were taken into account with the help of the multiple scattering approach by Wass, Rho, and Weise (WRW) [20].

The K^- in a nuclear bound state probes the K^- optical potential around the saturation density ρ_0, whereas experiments with kaonic atoms constrain reliably the K^- potential up to $\sim$ 50% of ρ_0 [12]. Beyond that limit the shape of the phenomenological multi-nucleon K^- potential in Eq. (1) results from extrapolation of the empirical formula to higher densities. Therefore, we considered two limiting options in our calculations. First, we took the full form of the phenomenological potential as is in Eq. (1) - full density option (FD). Then, we fixed the potential $V^{\rm phen}_{K^-{\rm multiN}}$ at constant value $V^{\rm phen}_{K^-{\rm multiN}}(0.5\rho_0)$ for $\rho(r) \geq 0.5\rho_0$ - half density limit (HD). In Table 2, we present $1s$ K^- binding energies B_{K^-} and corresponding widths Γ_{K^-}, calculated in the KM and P models for the two versions of the K^- multi-nucleon potential. For comparison, there are also binding energies and widths calculated only with the underlying K^- single-nucleon potential. When the K^- multi-nucleon processes are included the widths increase considerably while the binding energies change only slightly. For the FD option, the antikaon is not even bound in most of the nuclei due to very strong multi-nucleon absorption.

Table 2. 1s K^- binding energies B_{K^-} and corresponding widths Γ_{K^-} (in MeV) in various nuclei calculated using the single nucleon K^-N amplitudes (denoted KN); plus K^- multi-nucleon amplitude $B(\rho/\rho_0)^\alpha$, where $\alpha = 1$ and 2, for the HD and FD options (see text for details).

KM model			$\alpha = 1$		$\alpha = 2$	
		KN	HD	FD	HD	FD
^{16}O	B_{K^-}	45	34	not	48	not
	Γ_{K^-}	40	109	bound	121	bound
^{40}Ca	B_{K^-}	59	50	not	64	not
	Γ_{K^-}	37	113	bound	126	bound
^{208}Pb	B_{K^-}	78	64	33	80	53
	Γ_{K^-}	38	108	273	122	429
P model			$\alpha = 1$		$\alpha = 2$	
^{16}O	B_{K^-}	64	49	not	63	not
	Γ_{K^-}	25	94	bound	117	bound
^{40}Ca	B_{K^-}	81	67	not	82	not
	Γ_{K^-}	14	95	bound	120	bound
^{208}Pb	B_{K^-}	99	82	36	96	47
	Γ_{K^-}	14	92	302	117	412

4 Microscopic K^-NN absorption model and its application in kaonic atoms calculations

The absorption of K^- on two or more nucleons was found to be essential for a proper description of kaonic atoms data. So far, it was described mainly by a phenomenological optical potential which had to be extrapolated to the saturation density. Sekihara et al. [21]

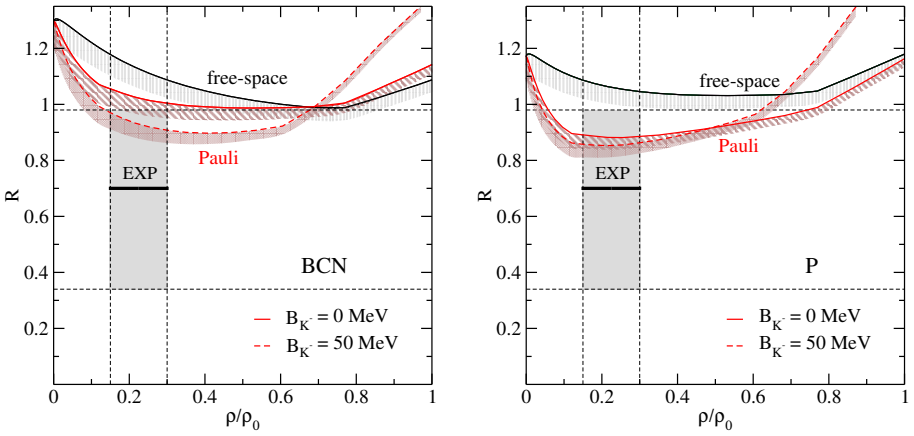

Figure 3. The ratio R as a function of relative density, calculated using the free-space and Pauli blocked amplitudes for $B_{K^-} = 0$ MeV and $B_{K^-} = 50$ MeV. Color bands denote the uncertainty due to different cut-off values $\Lambda_c = 800 - 1200$ MeV. Figure adapted from Ref. [23].

connected the two-nucleon antikaon absorption to chiral meson-baryon interaction models and developed the first microscopic model for K^-NN absorption in nuclear matter. Inspired by the evaluation of an η'-nucleus optical potential including η'-$2N$ absorption [22], we have developed a microscopic model for K^-NN processes in symmetric nuclear matter [23]. The description of K^- two-nucleon absorption was based on the meson-exchange picture. In the model, the scattering amplitudes derived from the Prague and Barcelona models were employed. We took into account the medium modifications of the free-space amplitudes due to the Pauli exclusion principle. We derived the real part of the K^-NN potential as well. Moreover, we derived the K^-N potential within the same approach. We built the total K^-N and K^-NN optical potentials as a sum of potentials coming from all possible absorption channels. For more details regarding the model see Ref. [23].

In order to test the validity of the K^-NN model, we calculated the ratio

$$R = \frac{\mathrm{BR}(K^- pp \to \Lambda p)}{\mathrm{BR}(K^- pp \to \Sigma^0 p)} = 0.7 \pm 0.2(\mathrm{stat.})^{+0.2}_{-0.3}(\mathrm{syst.})\,, \tag{2}$$

measured recently by the AMADEUS collaboration in reactions of low-energy K^- with carbon [24]. Figure 3 shows the ratio R as a function of relative density, calculated using free-space (black) and Pauli blocked (red) amplitudes derived from the BCN (left) and P (right) models. We performed calculations for two values of the kaon binding energy, $B_{K^-} = 0$ MeV (solid lines) and $B_{K^-} = 50$ MeV (dashed line). The AMADEUS experimental value including the error bar is denoted by the gray box and spans over the density area relevant for kaonic carbon. First, we evaluated the ratio using the free-space BCN and P model amplitudes. It lies above 1 and out of the gray box in the relevant density region. When the Pauli blocked amplitudes are taken into account, the value of the ratio drops down within the error bar of the experimental value. This result clearly illustrates the importance of in-medium modifications of the free-space amplitudes. More results of the K^-NN model can be found in Ref. [23].

As the next step, we applied the microscopic K^-NN model in kaonic atoms calculations to test further its validity [25]. We calculated the microscopic $K^-N + K^-NN$ potentials for 23 nuclear targets and confronted them with kaonic atom data. Next, we added a phenomeno-

Table 3. Values of $\chi^2(65)$ resulting from the comparison of the calculations of kaonic atoms using K^-N, $K^-N + K^-NN$, and $K^-N + K^-NN$+phen. multi-nucleon potentials based on the Pauli blocked and WRW modified BCN amplitudes with the experimental data. Values of complex amplitude B and parameter α are presented as well.

	K^-N	$K^-N + K^-NN$	+ phen.	ReB (fm)	ImB (fm)	α
Pauli	825	565	105	-1.97(13)	-0.93(11)	1.4
WRW	2378	1123	116	-0.90(9)	0.72(10)	0.6

logical term $\sim B(\frac{\rho}{\rho_0})^\alpha\rho$ to the $K^-N + K^-NN$ potentials to quantify the effect of K^--$3N(4N)$ processes which are missing in the microscopic model. In the calculations, we employed the BCN and P model amplitudes and considered their in-medium modification due to the Pauli exclusion principle within two approaches: 1) the Pauli blocked amplitudes were evaluated directly in the chiral model (denoted by 'Pauli') 2) we employed the multiple scattering approach WRW [20].

In Table 3, the values of $\chi^2(65)$ resulting from the comparison of predictions of K^-N, $K^-N + K^-NN$, and $K^-N + K^-NN$+phen. potentials with kaonic atoms data are presented. The description of the data improves significantly when the K^-NN absorption is taken into account, the value of $\chi^2(65)$ decreases to about one half, however, it is still considerable. When the additional phenomenological term is added to the $K^-N + K^-NN$ potentials, values of $\chi^2(65)$ further decrease to $\sim$ 100 and become comparable with the best fit K^-N+phenomenological potential, ReB = -1.3 fm, ImB = 1.9 fm, α = 1, $\chi^2(65)$ = 112.3. The values of the complex amplitude B and the parameter α fitted to the data are presented as well. For the Pauli blocked amplitudes, the value of ImB of the additional phenomenological term is negative. The $K^-N + K^-NN$ potentials thus seem to be too absorptive with no space for additional absorption from $3N(4N)$ processes. The potentials based on the WRW amplitudes yield positive ImB = 0.72 fm, being about half of the value of the amplitude obtained with the best fit K^-N+ phen. multi-nucleon potential, which seems reasonable. The parameter α controls the density dependence of the additional phenomenological term. For the description of $3N(4N)$ processes, it is expected $\alpha \geq 2$. The fit yields values of α lower than 2 in both cases. The above results indicate some deficiencies in the microscopic K^- potentials which need to be resolved. A possible solution could be a proper inclusion of the hadron self-energies, which are part of the medium modifications, in the K^-NN model as well as in the K^-N chiral amplitudes. They were not considered in the present calculations, however, an extension of the model to involve the hadron self-energies is currently under investigation.

5 Summary

In this contribution, we reviewed the current status of the K^-N and K^--nuclear interactions derived from the SU(3) chiral meson-baryon interaction models. The K^- single-nucleon potentials based on chiral K^-N scattering amplitudes are unable to describe kaonic atoms data on their own. It turned out that an indispensable ingredient of the K^--nuclear interaction is the K^- absorption on two and more nucleons. After supplementing the K^-N chiral potentials by a phenomenological density-dependent multi-nucleon term, the description of the data significantly improves, yielding the value χ^2/d.p.$\leq$ 2 for all state-of-the-art chiral models. Moreover, only the P, KM, and BCN models were found compatible with kaonic atoms data and the value of the K^- single-nucleon absorption fraction deduced from bubble chamber experiments. The K^-N chiral + phen. multi-nucleon potentials based on the P and KM models were applied in the calculations of K^--nuclear quasibound states in many-body systems

($A \geq 6$). The strong multi-nucleon absorption caused the K^- widths to be up to order of magnitude larger than the corresponding binding energies. In some nuclei, depending on the form of the phenomenological multi-nucleon potential applied at saturation density, the K^- was found even unbound.

Next, we developed a microscopic model for the K^-NN absorption in nuclear matter. The model was applied in the kaonic atoms calculations for the first time. The description of the data significantly improved when the microscopic K^-NN potential was added to the K^- single-nucleon potential derived from the BCN chiral amplitudes. However, the values of $\chi^2(65)$ were still sizeable suggesting that some processes of K^--$3N(4N)$ absorption are missing. Therefore, we added a phenomenological term to the $K^-N + K^-NN$ microscopic potentials to quantify the $3N(4N)$ processes. The unexpected density dependence of the additional phenomenological term revealed some deficiencies in the microscopic potentials. Further improvements, i.e. proper inclusion of hadron self-energies in the K^-N chiral amplitudes, of the microscopic $K^-N + K^-NN$ potentials are thus desirable.

Acknowledgements

J.O. and J.M. acknowledge support from the GACR Grant No. 19-19640S. J.O. acknowledge partial support from the project of the European Regional Development Fund No. CZ.02.1.01/0.0/0.0/16 019/0000778. A.R. acknowledges support from the grants CEX2019-00098-M and PID2020-118758GB-100 of the AEI (Spain). This work is also part of a project funded by the European Union's Horizon 2020 research & innovation programme, grant agreement 824093.

References

[1] A. D. Martin, Nucl. Phys. **B 179**, 33 (1981)
[2] J. Ciborowski *et al.*, J. Phys. **G 8**, 13 (1982)
[3] D. Evans *et al.*, J. Phys. **G 9**, 885 (1983)
[4] D. N. Tovee *et al.*, Nucl. Phys. **B 33**, 493 (1971)
[5] R. J. Nowak *et al.*, Nucl. Phys. **B 139**, 61 (1978)
[6] M. Bazzi *et al.* (SIDDHARTA collaboration), Phys. Lett. **B 704**, 113 (2011); Nucl. Phys. **A 881**, 88 (2012)
[7] A. Cieplý, J. Smejkal, Nucl. Phys. **A 881**, 115 (2012)
[8] Y. Ikeda, T. Hyodo, W. Weise, Nucl. Phys. **A 881**, 98 (2012)
[9] Z. H. Guo, J. A. Oller, Phys. Rev. **C 87**, 035202 (2013)
[10] M. Mai, U.-G. Meißner, Nucl. Phys. **A 900**, 51 (2013)
[11] A. Feijoo, V. Magas, À. Ramos, Phys. Rev. **C 99**, 035211 (2019)
[12] E. Friedman, A. Gal, Nucl. Phys. **A 959**, 66 (2017)
[13] H. Davis *et al.*, Nuovo Cimento **53 A**, 313 (1968)
[14] J. W. Moulder *et al.*, Nucl. Phys. **B 35**, 332 (1971)
[15] C. Vander Velde-Wilquet *et al.*, Nuovo Cimento **39 A**, 538 (1977)
[16] K. Piscicchia, S. Wycech, L. Fabbietti *et al.*, Phys. Lett. **B 782**, 339 (2018)
[17] W. Weise, Nucl. Phys. **A 835**, 51 (2010), and references therein
[18] J. Hrtánková, J. Mareš, Phys. Lett. **B 770**, 342 (2017)
[19] J. Hrtánková, J. Mareš, Phys. Rev. **C 96**, 015205 (2017)
[20] T. Wass, M. Rho, W. Weise, Nucl. Phys. **A 617**, 449 (1997)
[21] T. Sekihara *et al.*, Phys. Rev. **C 86**, 065205 (2012)

[22] H. Nagahiro *et al.*, Phys. Lett. **B 709**, 87 (2012)
[23] J. Hrtánková, À. Ramos, Phys. Rev. **C 101**, 035204 (2020)
[24] R. Del Grande *et al.*, Eur. Phys. J. **C 79**, 190 (2019)
[25] J. Óbertová, E. Friedman, J. Mareš, preprint submitted to Phys. Rev. **C**, (2022), arXiv:2208.14946 [nucl-th]